American Mineralogist, Volume 58, pages 116-127, 1973

Kogarkoite, a New Natural Phase in the System Na_2SO_4-NaF-NaCl

ADOLF PABST, *Department of Geology and Geophysics, University of California, Berkeley, California 94720*

AND

WILLIAM N. SHARP, *U.S. Geological Survey, Denver, Colorado 80225*

Abstract

"Chlorine-free schairerite" was described from the Lovozero massif, Kola Peninsula, USSR, by Kogarko in 1961. A constituent of white sublimate formed at Hortense Hot Spring, Colorado, was found by W. N. Sharp in 1970 to yield an "X-ray powder pattern similar to that of the multiple salt Na_2SO_4NaF. . . ." Both materials are identical with synthetic Na_3SO_4F, first described by de Marignac in 1859.

The name kogarkoite has been selected for the newly recognized mineral. Though the other multiple salts in the system—schairerite, galeite, and sulfohalite—are known only from evaporites, kogarkoite is found in igneous associations of two distinct sorts. In nepheline syenites of the Kola, it occurs with villiaumite and doubtless formed at relatively high temperature. In Colorado, kogarkoite formed at 83°C or less in hot-spring sublimate, and its principal associates are calcite, fluorite and opal.

Kogarkoite is monoclinic, space group $P2_1/m$ or $P2_1$; a 18.073 Å, b 6.949, c 11.440, β 107°43′, $Z = 12$; density (calc) 2.679, (meas. by Berman balance on fragments grown from melt) 2.676; optically almost uniaxial positive; refractive indices are $\alpha \approx \beta = 1.439$, $\gamma = 1.422$, Z axis $\parallel$ [$\bar{1}$02]. Morphologically, crystals appear to be rhombohedral showing a prominent base, which is the monoclinic {101}, and several apparent rhombohedra. The pseudorhombohedral character arises from submicroscopic intergrowth of monoclinic domains in three orientations. The atomic arrangement in a subcell is similar to that in sulfohalite.

Introduction

With the recent discovery of kogarkoite (Na_3SO_4F) in Colorado and verification of a find in Russia, the naturally occurring multiple salts in the system Na_2SO_4–NaF–NaCl now include this mineral, schairerite ($Na_{21}(SO_4)_7F_6Cl$), galeite ($Na_{15}(SO_4)_5F_4Cl$), and sulfohalite ($Na_6(SO_4)_2FCl$).

A sodium fluoride sulfate was first recognized in laboratory-prepared material and described by de Marignac (1859). Later Wolters (1910) dealt with it in the dry system Na_2SO_4–NaF–NaCl, and Foote and Schairer (1930) in the hydrous system Na_2SO_4–NaF–NaCl–H_2O. They concluded that "At these temperatures (25–35°) the double salt, Na_2SO_4–NaF, forms a solid solution in which the fluoride is replaced by chloride to a limited extent." However, this statement was based entirely on analyses of "residues" (Foote and Schairer, 1930, p. 4211) without proof of the absence of free solid NaCl in those samples in which the analytically determined amount was low. Foshag (1931) described schairerite from the Searles Lake evaporites, and formulated it as $Na_2SO_4 \cdot Na(F, Cl)$. He referred to the artificial "double salt," $Na_2SO_4 \cdot NaF$, described by Schairer, as artificial schairerite in spite of the fact, which he noted, that it is of "totally different habit."

Kogarko (1961), following these precedents, referred to a mineral of composition Na_3SO_4F, found in nepheline syenites at Lovozero on the Kola Peninsula, as "chlorine-free schairerite." Her paper describes the first known natural occurrence of the mineral, and because of this the name, kogarkoite, was proposed to and accepted by the I.M.A. Commission on New Minerals and Mineral Names of the International Mineralogical Association.

Soon thereafter, Pabst, Sawyer, and Switzer (1963) gave full morphological, chemical, optical, and X-ray data on the artificial kogarkoite and on the related minerals schairerite, galeite, and sulfohalite. At the time, they were unaware of the work of Kogarko. They also unwisely used Foshag's formula for schairerite and used the same formula for

galeite, though notes with their Tables 1 and 3 and discussion on pages 498 and 499 made it clear that fixed F:Cl ratios, 6:1 and 4:1, were indicated for schairerite and galeite respectively.

Brown and Pabst (1971) show that microprobe analyses of schairerite, of galeite, and of schairerite–galeite polycrystals fully support the suggestions of Pabst *et al.* (1963, p. 499), and these data indicate that the following formulas are appropriate:

Schairerite	$Na_{21}(SO_4)_7F_6Cl$
Galeite	$Na_{15}(SO_4)_5F_4Cl$

The misleading double salt formulation, $Na_2SO_4 \cdot Na(F, Cl)$, should no longer be used for these minerals.

Pabst *et al.* (1963, Table 7) published indexed powder patterns of all the multiple salts in the system Na_2SO_4–NaF–NaCl. The Colorado kogarkoite pattern is identical to these Na_3SO_4F diffraction data. Comparison of Kogarko's X-ray tabulation for "chlorine-free schairerite from Lovozero" and for the artificial "double salt" with corresponding parts of Table 7 shows that the powder pattern of the mineral from the Kola Peninsula does not exactly agree with that of either schairerite or the artificial "double salt" but is closer to the latter. Moreover, from the analysis and optical properties reported by Kogarko it is clear that she was dealing with the "double salt" and *not* with schairerite.

One of us (Sharp, 1970) recently found the double salt with opal and a variety of other minerals in hot-spring deposits at Mt. Princeton Hot Springs, Colorado.

Occurrence

The occurrence in the Lovozero Massif, Kola Peninsula, as described by Kogarko (1961), is in nepheline syenite pegmatite, closely associated and at places intergrown with villiaumite (NaF).

Other associated minerals are nepheline, feldspar, aegirine, ramsayite, apatite, and lamprophyllite. The kogarkoite is pale blue, and occurs as grains and aggregates occupying interstices between nepheline and feldspar.

This occurrence, to say the least, is uncommon —as is the villiaumite found associated with it and in most of the various rocks of this massif. The situation for formation of these minerals seems clearly to be late-stage crystallization at a temperature near the critical temperature for water in the system—where these compounds are virtually insoluble (Kogarko, 1961).

Kogarkoite occurs in Colorado in a repeatedly generated, white, punky sublimate around steaming vents at several of the issues of hot-spring water at Mt. Princeton Hot Springs along Chalk Creek in Chaffee County. The hot springs area is also conspicuous because of the prominent chalky bluffs on the flanks of the mountain mass above the spring zone. Large masses of shattered quartz monzonite are extensively zeolitized and have formed the Chalk Cliffs upon erosion. The present hot springs are considered residual issues in a thermal area of long duration (Sharp, 1970).

Specifically, kogarkoite has been found only at Hortense Hot Springs at the west edge of the thermally active area and at wells drilled close by. The principal spring has a modest flow of water at the present surface site where water is of the highest temperature for the area, 183°F. Water from two wells drilled to depths of 150+ feet near the Hortense natural issue is equally hot. Hortense Spring is located high above the valley floor, at the top of the valley-wall fans, immediately under the steep zeolitized rock cliffs. At present, polymineralic sublimate crusts form from steam issuing from flowing hot water. Piping is used to transport the water from underground into a collecting concrete cistern. A port in the pipe, open to the air, and the hole in the cistern receiving the pipe both have white salt incrustations. Any steam-venting orifice at the drilled well installations nearby also develops mineral incrustations. Rocks scattered about the old Hortense surface site—now bulldozed level for development —are coated with a crust of durable minerals—calcite, fluorite, and opal—an assemblage which must have initially included the soluble phases.

Kogarkoite occurs in all the vent crust found at Hortense and at the drilled wells close by. The incrustations form only at the opening edge—neither inside the cavity nor more than a few inches outside, depending apparently on the force and amount of steam. The conditions for sublimation seem delicately limited to temperature, degree of saturation and composition of the steaming issue. Also, the punky opal sublimate may be a required host in which fluids accumulate and reach required component concentrations for the formulation of kogarkoite.

Analysis of water from Hortense shows high values for SiO_2, Na, SO_4, F, and HCO_3 with total dis-

solved solids of 339 ppm. Complete chemical and spectrographic analyses are given by Sharp (Table 2, 1970). Other springs in the Mt. Princeton Hot Springs group—Haywood Hot Springs (100°F), and Big Spring (130°F)—may produce sublimate products similar to Hortense Springs; however, these springs are generally developed for use of the hot water and access to original sites and new water vents is difficult.

Association

The incrustations at Hortense Spring and at Wright's well are exceedingly fine grained and somewhat inhomogeneous. Opal, mostly milky, is the principal constitutent and is easily recognized by its characteristic shapes, commonly minutely tubular or banded with smoothly rounded surfaces except where intimately mixed with other minerals. The only crystalline phase that can be readily recognized under a microscope is kogarkoite. This occurs in small clusters or single crystals as much as 0.7 mm in maximum dimensions but mostly in the range 0.1–0.3 mm.

The remaining constituents are mostly so fine grained as to yield smooth powder diffraction lines without crushing or grinding. A powder pattern of a bulk sample would be difficult to interpret because of the large number of diffracting phases, but burkeite, trona, halite, fluorite, calcite, and kogarkoite were readily identified in two or more of the pieces tested. Fluorite lines are generally broad and diffuse indicating very small grain size, whereas the lines due to other constituents are mostly sharp and well defined as in ordinary powder patterns.

Portions of two samples from Hortense Spring were leached with distilled water for several days each and found to contain 20 and 37 percent respectively of water-soluble constitutents. The principal crystalline constituent in the residue is calcite. A few lines attributable to phillipsite were also registered from one of the samples.

The solutions obtained by water-leaching were crystallized. The crystallized product consisted of powdery white halite with scattered clear spots or rosettes, mostly kogarkoite and some trona.

It seems probable that the incrustations consist of about 60 percent opal, 20 percent calcite and a few percent of each of the other minerals identified, kogarkoite being the chief among these, plus traces of detrital material and unidentified phases.

Lattice and Symmetry

In view of the uncertainty that has existed concerning the symmetry of Na_3SO_4F it will be necessary to clarify this before describing the morphology and properties of kogarkoite and its synthetic counterpart. Originally, de Marignac (1859, p. 236) found the tiny crystals to be curved and striated and was unable to obtain an interference figure. Though he gave the "forme primitive" as "rhomboèdre?," he listed five forms for which Miller–Bravais indices were assigned by Groth (1908, p. 376) and nine pairs of observed and calculated interfacial angles, and presented a crystal drawing. Wolters (1910, p. 66) grew crystals of Na_3SO_4F from aqueous solution at 35°C and confirmed the observations of de Marignac but was able to obtain a "nearly uniaxial" positive interference figure. Additionally he noted sets of fine lines intersecting at 60° in thin sections of Na_3SO_4F grown from a melt. These he ascribed to an ultrafine complicated mimetic twin structure. The disappearance of these lines, as well as other optical changes upon heating and the detection of a small discontinuity on the cooling curve at 105°C, was interpreted by Wolters as indicating that Na_3SO_4F is truly hexagonal only above this temperature.

Foote and Schairer (1930, p. 4206) reported that the synthetic crystals are "tabular with hexagonal outline and decided trigonal symmetry." Foshag (1931, p. 136–137) erroneously referred to the Na_3SO_4F prepared by Schairer as artificial "schairerite" and published a drawing of it—a tabular crystal with base and two rhombohedra, "of a totally different habit" from natural schairerite. Kogarko (1961) did not comment on the crystallography of the natural material which she described as "chlorine-free schairerite."

A rhombohedral lattice was first assigned to Na_3SO_4F by Pabst, Sawyer and Switzer (1963), and the morphology reported by earlier observers reconciled with this lattice. However, in an extended section of that publication entitled "Complications in $Na_2SO_4 \cdot NaF$," single crystal X–ray evidence for lower symmetry was cited, and it was concluded that "The structure cannot have a Laue symmetry higher than $2/m$ though the lattice is dimensionally rhombohedral." At that time certain minor features of Weissenberg patterns which do indicate a slight dimensional departure from strictly rhombohedral relations were not noticed or were disregarded.

Powder patterns can be fully indexed on a rhombo-

hedral lattice. Rotation patterns (Fig. 1) on the apparent c axis show to perfection the systematic absences required by a rhombohedral lattice. The indications of lower symmetry recognized earlier were principally the variations in intensity distribution on $hki0$ precession patterns. However, close inspection of the high 2θ region of Weissenberg patterns shows triplets for many spots, especially the stronger spots, in places where only the $K_{\alpha 1}$–$K_{\alpha 2}$ doublets would be expected. Measurement of $hk\bar{i}0$ and $h0\bar{h}l$ quartz–calibrated Weissenberg patterns and attempts to select appropriate components of the triplets led to consistent values for c but to a scattering of values for a over a range of about 1/500th of its value. Eventually one of the synthetic crystals that had been used in the earlier work was found to yield patterns free of such triplets. It was also found that some of the patterns obtained from the Russian kogarkoite were nearly free of such disturbing features. Table 1 gives lattice dimensions obtained from these patterns. The dimensions obtained for the synthetic crystal by least squares from two quartz–calibrated Weissenberg patterns, with σ of 0.035 percent and 0.011 percent and with a difference of the common value between the two of 0.0024 percent, are better than those obtained from shrinkage–corrected precession patterns for the Russian kogarkoite. Even so, the former values are well within the limits of error assigned to the latter. Table 1 also gives the hexagonal and rhombohedral cell dimensions corresponding to the pseudorhombohedral lattice, obtained by least squares from six lines free of superposition on a quartz–calibrated powder pattern run with Cr–V radiation. Though σ is somewhat higher than for the calculations from Weissenberg data, it is acceptable for data of this sort where high–angle lines cannot be used.

Figure 2 shows the relations of the monoclinic lattice to the pseudorhombohedral lattice just mentioned and to a small pseudorhombohedral subcell to be considered later. The correspondence of the sides of the monoclinic to the hexagonal cell are as follows: (100) (10$\bar{1}$1); (010) ($\bar{2}$4$\bar{2}$0); (001) ($\bar{1}$0$\bar{1}$2); and vice versa: (30$\bar{3}$0) (20$\bar{1}$); ($\bar{2}$4$\bar{2}$0) (010); (0003) (101). The relations between the two lattices can be defined by the matrices for transforming indices of faces or planes: monoclinic to hexagonal $1\bar{2}\bar{1}/040/102$ and hexagonal to monoclinic $\frac{2}{3}\ \frac{1}{3}\ \frac{1}{3}/0\ \frac{1}{4}\ 0/\frac{1}{3}\ \frac{1}{6}\ \frac{1}{3}$. Figure 3 shows the correspondence of monoclinic indexing to hexagonal indexing for all of the principal forms observed on natural and synthetic kogarkoite. These relations are

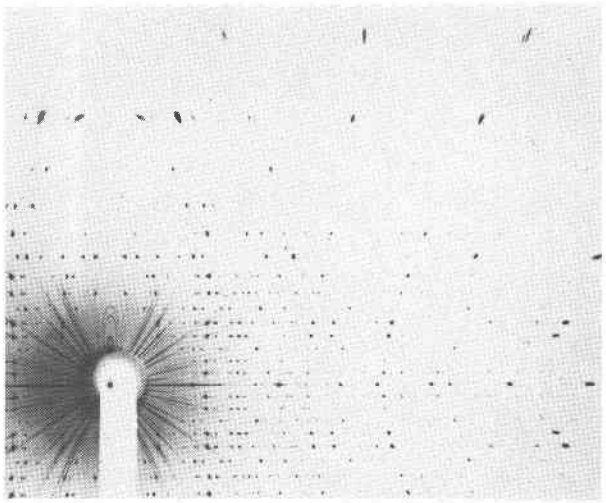

FIG. 1. The X–ray rotation pattern of a kogarkoite crystal grown from solution at 38°C. Cu radiation, Ni filter. Rotation axis [102] monoclinic, corresponding to c pseudohexagonal. c^* streaks visible adjacent to strong spots on $80\bar{8}l$ locus on which spots appear only on layer lines for which $l \neq 3n$ in accordance with requirements of rhombohedral centering.

not exact but the departure is so slight that it ordinarily escapes notice. The [102] monoclinic axis is taken as the c hexagonal axis and should be normal to the (101) monoclinic plane which is taken as the (00.3) hexagonal plane. However, the angle between these is 90° 11 1/2′, as calculated from the monoclinic cell dimensions. Also, the angle between the monoclinic [010] and [$\bar{1}$21] axes, corresponding to the hexagonal a_1 and a_2 axes, is 60° 4 1/2′.

TABLE 1. CELL DIMENSIONS OF Na_3SO_4F AND KOGARKOITE

	1	2	3		
$\underline{a}$	18.073(7) Å	18.066(20)	$\underline{a}_h$	27.850(16)	$\underline{a}_r$ 18.027
$\underline{b}$	6.9489(7)	6.952(12)	$\underline{c}_h$	24.453(14)	α 78° 51′
$\underline{c}$	11.440(4)	11.438(12)			
β	107° 43′	107° 38′			
Z	12	12	144		48
d(calc.)	2.6790+		2.6791+		

Notes:

1. Dimensions for kogarkoite grown from solution, obtained from quartz-calibrated Weissenberg patterns by least squares.
2. Dimensions for kogarkoite from the Lovozero massif, obtained from shrinkage-corrected precession patterns.
3. Dimensions of hexagonal and rhombohedral pseudocells, obtained from powder diffraction patterns of kogarkoite.

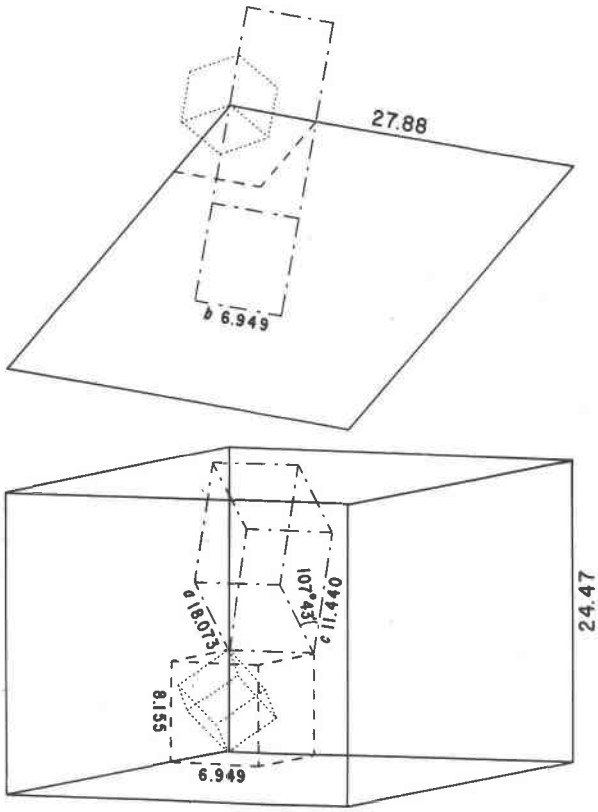

FIG. 2. Relations between monoclinic unit cell and pseudocells of kogarkoite. Top view is projection onto (101), which corresponds to (0001) pseudohexagonal. Dash–dot lines outline monoclinic cell; full lines large hexagonal pseudocell; dotted lines rhomobohedral subcell and dashed lines the hexagonal cell corresponding to this subcell. Compare Fig. 7 (Pabst, Sawyer, and Switzer, 1963).

Table 2 records the powder pattern used for redetermining the dimensions of the pseudohexagonal cell. Dual indexing is given. All hexagonal indices conform to the rhombohedral lattice requirements, with the additional restriction that $k = 4n$, which arises from the relations defined by the matrices given above. A given hexagonal form may correspond to one, two, or three monoclinic forms and so may be recorded several times. For instance, $\{44\bar{8}9\}$ is represented in the table by (711) $(44\bar{8}9)$, (323) $(\bar{4}8\bar{4}9)$ and $(\bar{1}15)$ $(\bar{8}449)$, with monoclinic spacing differing by as much as 0.0050. This table corresponds in large measure to the previously published record for Na_3SO_4F (Pabst, Sawyer, and Switzer, 1963, Table 7, also ASTM–PDF card 15–678). However, that tabulation lacked the multiple indexing.

Figures 4A and 4B show precession patterns of Lovozero kogarkoite on the monoclinic [010] and $[\bar{1}21]$ axes respectively. Dial axis settings with the pseudorhombohedral c axis as common axis were 60° apart, and the slight missetting, ± 4 1/2′, is not detectable. The distribution of spots on both patterns is that expected with a rhombohedral lattice in $(h0\bar{h}l)$ and $0hh\bar{l}l$) sections, spots with $h \neq 4n$ being weak in the former and absent in the latter. Except for these weaker spots the patterns are identical. Precession patterns on the hexagonal a_1, a_2, and a_3 axes (monoclinic $[\bar{1}21]$, [010] and $[12\bar{1}]$) were run on several crystals. In only two crystals were the weak spots with $h \neq 4n$ absent on the a_1 and a_3 precession patterns. In others they were present on all three, usually with varying intensity relations, in a few cases with identical intensity relations as would be expected in a truly rhombohedral material.

These findings and other peculiarities of the diffraction effects can be explained by the presence within the apparently single crystals of domains related by 120° and 240° rotations about the monoclinic [102] axis and thus giving rise to an apparently trigonal axis, the hexagonal c. In the X–ray patterns from such composite edifices, reciprocal lattice sections such as those of Figures 4A and 4B would be superposed, the match being very good because (101) [= (0003)] is in common for the two and because d for (201) [= $(30\bar{3}0)$]

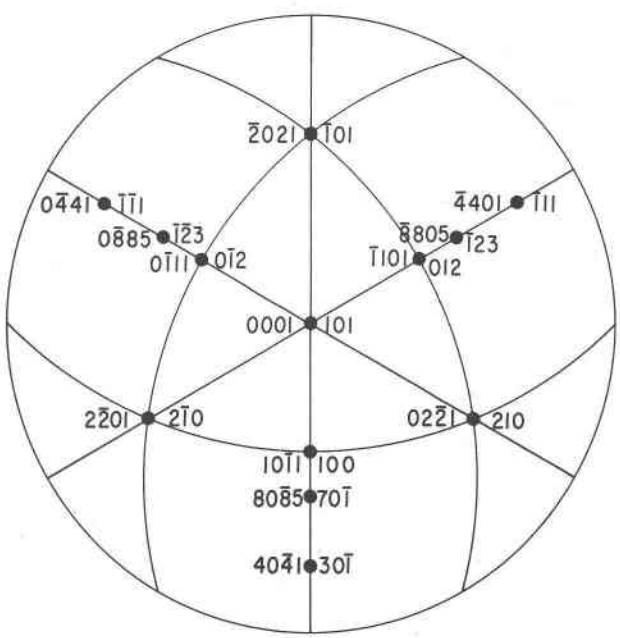

FIG. 3. Stereographic projection of forms recorded on kogarkoite. Plane of projection (101) monoclinic, corresponding to (0001) pseudohexagonal. Both monoclinic and hexagonal indices are given for each plane.

is 8.051 and differs by only 1/400 from the d spacing of 2.0077 or 8.031/4 for $(43\bar{2})$ [$=(01\bar{1}0)$].

In precession patterns so slight a misfit is barely perceptible if a very small crystal is used and settings are precise. However, the discrepancy is of the same order of magnitude as the difference between Cu $K\alpha_1$ and $K\alpha_2$ wavelengths. This gives rise to the triplets in the high 2θ region of Weissenberg patterns, previously mentioned. An example is given in Figures 5A and 5B which show small sections of the [102] zero layer (hexagonal c zero layer of $hki0$) Weissenberg patterns for a simple monoclinic crystal and for a more typical intergrown crystal that gives rise to the triplets. The detailed explanation is given under the figures. For all crystals except one grown from solution at room temperature, triplets such as those shown in Figure 5B are seen in the high 2θ regions of zero and higher layer Weissenberg films, regardless of axis of rotation; however, in a few crystals such as that represented by the precession patterns in Figures 4A and 4B, the intergrowth is not fully random in three orientations. However, triplets or other multiplets are not seen for $(000l)$ or for other spots for which $h \neq 4n$ when indexed on the large hexagonal cell.

Heavily exposed films such as the rotation pattern shown in Figure 1 sometimes show streaks parallel to c^* (pseudohexagonal) along the most prominent reciprocal lattice rows. This would suggest stacking errors—in this case irregular sequences of the three orientations of the monoclinic structure which simulate a rhombohedral lattice when perfectly random.

TABLE 2. X-RAY POWDER DIFFRACTION DATA FOR KOGARKOITE

I	hkl	hkil	d(obs.)	d(calc.) monoc.	d(calc.) hex.	I	hkl	hkil	d(obs.)	d(calc.) monoc.	d(calc.) hex.
50	400	40.4	4.29 2/	4.303	4.293		610	44.6		2.652	
	012	$\bar{4}4.4$		4.288		15	$\bar{2}14$	$\bar{8}4.6$	2.648 2/	2.645	2.647
70	311	04.5	3.80 2/	3.802	3.798		222	$\bar{4}8.6$		2.645	
	$\bar{1}03$	$\bar{4}0.5$		3.797			$\bar{4}22$	$\bar{1}08.0$		2.631	
	401	30.6		3.643			502	30.9		2.578	
5	003	$\bar{3}0.6$	3.63	3.633		25	$\bar{7}01$	$\bar{8}0.\bar{5}$	2.572	2.573	
	$\bar{5}01$	60.3		3.616			104	$\bar{3}0.9$		2.573	
	$\bar{3}03$	$60.\bar{3}$		3.605		70	$\bar{1}23$	$\bar{8}8.5$	2.564 1/	2.563	2.566
100	$\bar{4}12$	$\bar{8}4.0$	3.48 2/	3.484	3.481		313	$\bar{2}4.9$		2.532	
	020	$\bar{4}8.0$		3.475		5	$\bar{4}14$	$\bar{1}04.4$	2.520	2.520	
10	103	$\bar{2}0.7$	3.36	3.355		30	403	10.10	2.431 1/	2.436	2.433
	411	14.6		3.226		10	521	08.7	2.281	2.283	
	$01\bar{3}$	$14.\bar{6}$		3.219			$\bar{3}05$	$\bar{8}0.7$		2.281	
3d	$\bar{5}11$	$\bar{8}4.3$	3.21	3.207		10	$\bar{1}24$	$\bar{9}8.7$	2.191	2.193	
	$\bar{3}13$	$\bar{8}4.\bar{3}$		3.200			$\bar{3}24$	$\bar{1}\bar{1}8.7$		2.188	
	121	$\bar{4}8.3$		3.197			$\bar{3}31$	$2\bar{1}2.\bar{1}$		2.1545	
	203	$\bar{1}0.8$		3.033		30	800	80.8	2.1495	2.1521	
3	501	40.7	3.03	3.029			024	$\bar{8}8.8$		2.1440	
	113	44.7		3.021		85	711	44.9	2.1419 1/	2.1460	2.1426
85	$\bar{5}03$	$\bar{8}0.1$	2.991 2/	2.995	2.992		323	$\bar{4}8.9$		2.1410	
	$\bar{3}21$	$\bar{8}8.1$		2.990			$\bar{1}15$	$\bar{8}4.9$		2.1410	
20	$\bar{6}02$	$\bar{8}0.2$	2.927 2/	2.933	2.927	25	$\bar{7}05$	$120.\bar{3}$	1.9521 1/	1.9515	1.9515
	$\bar{2}22$	$\bar{8}8.2$		2.923			$\bar{5}31$	$\bar{1}\bar{2}12.3$		1.9502	
5	122	$\bar{5}8.5$	2.814	2.813		25	622	08.10	1.9005 1/	1.9004	1.8992
85	303	00.9	2.718 2/	2.719	2.717		$20\bar{6}$	$80.\bar{1}0$		1.8985	
85	420	08.4	2.705 2/	2.704	2.704	15	$10.0.\bar{2}$	120.6	1.8022 1/	1.8078	1.8026
	$40\bar{4}$	$80.\bar{4}$		2.704			$23\bar{4}$	$012.\bar{6}$		1.8000	
	$\bar{6}12$	$\bar{1}04.\bar{2}$		2.703							

Notes:

The table is based on a pair of powder patterns made with V-filtered, Cr radiation, in a camera with 114.59 mm diameter, one with and one without quartz calibration.

1/ Indicates lines used for the least squares calculation of the dimensions of the pseudohexagonal cell. For these lines $\sigma = 0.060$ percent.

2/ Indicates lines used for a check on the dimensions of the pseudohexagonal cell. For these lines $\sigma = 0.057$ percent.

Spacings calculated from the hexagonal cell dimensions are given only for lines of these two groups. Indices and monoclinic calculated spacings are given for all planes considered to contribute to the recorded lines. Within the range of spacings to 1.8 Å there are nearly 200 more not corresponding to recorded lines.

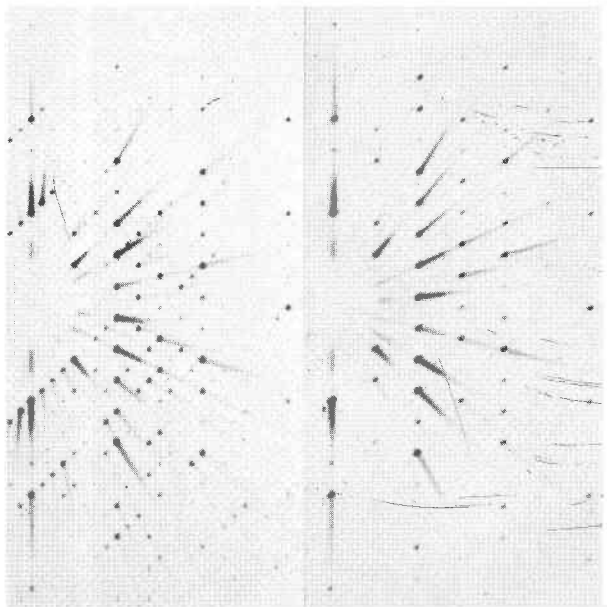

A B

FIG. 4A and 4B. Mo–Zr, zero level precession patterns of kogarkoite from the Lovozero massif. The [102] monoclinic, c pseudohexagonal, axis is vertical in both patterns.

A (left). Precession axis [010].

B (right). Precession axis [$\bar{1}$21].

Space Group and Cell Content

The only systematic monoclinic absences are $(0k0)$ for $k \neq 2n$. This suggests that the space group is $P2_1$ or $P2_1/m$. However, in rhombohedral indexing, $hh\bar{2}\bar{h}l$ reflections appear only for $h = 4n$. This includes the monoclinic systematic absence just mentioned, so it may be that this is a consequence of the pseudo-rhombohedral character of the structure.

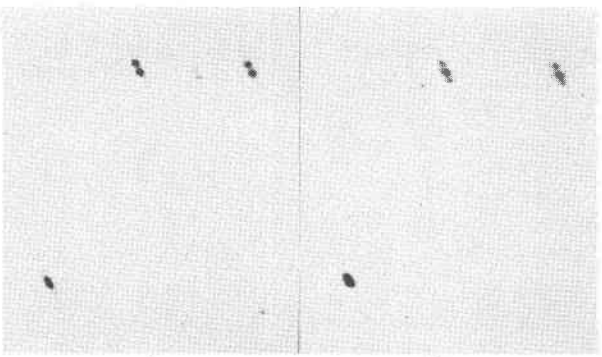

FIG. 5A and 5B. Enlargements of small sections of the high angle regions of [102] (monoclinic), *c* (pseudohexagonal), zero-layer Weissenberg patterns of kogarkoite.

A. Truly monoclinic single crystal, showing the spots from left to right:

monoclinic	"hexagonal"	*d*
080	$\bar{1}\bar{6}.32.\bar{1}\bar{6}.0$	0.86825 Å
884	$\bar{4}.32.\bar{2}\bar{8}.0$	0.79753
$12.7.\bar{6}$	4.28.32.0	0.79806

B. Intergrown crystal with pseudohexagonal development, showing same spots plus overlapping spots:

monoclinic	"hexagonal"	*d*
16.4.8	$16.16.\bar{3}\bar{2}.0$	0.87083
20.1.10	$28.4.\bar{3}\bar{2}.0$	0.79977

The overlapping of spots in B gives rise to triplets because the difference in *d* of the overlapping spots, about 0.28 percent, is nearly the same as the difference in wavelength of CuKα_1 and CuKα_2, 0.25 percent.

TABLE 3. MODIFIED MONOCLINIC ANGLE TABLE FOR KOGARKOITE

$a : b : c = 2.6008 : 1 : 1.6463$; β 107° 43'; $p_o : q_o : r_o = 0.6330 : 1.5683 : 1$

$r_2 : p_2 : q_2 = 0.4036 : 0.6376 : 1$; 72°17'; p_o' 0.6645, q_o' 1.6463, x_o' 0.3193

				"c"	
$hk\bar{i}l$	hkl	ϕ	ρ	$(hkl \wedge 101)$	$(h0\bar{h}l \wedge 0001)$
$\bar{1}011$ [1]	001	90° 00'	17° 43'		from hexagonal constants for rhombohedral pseudocell
0001	101	90° 00'	44° 32'		
$\bar{1}010$ [1]	$\bar{2}01$	90° 00'	-45° 16 1/2'	89° 48 1/2' [2]	90° 00'
$02\bar{2}1$	210	38° 55'	90° 00'	63° 52'	63° 45'
$\bar{2}02l$	$\bar{1}01$	90° 00'	-19° 03'	63° 35'	
$\bar{4}041$	$\bar{3}01$	90° 00'	-59° 09'	76° 19'	76° 09'
$\bar{4}401$	$\bar{1}11$	-11° 50'	59° 16'	76° 05'	
$10\bar{1}1$	100	90° 00'	90° 00'	45° 32'	45° 23'
$\bar{1}101$	012	22° 49'	41° 26'	45° 23'	
$\bar{8}08\bar{5}$	$\bar{7}01$	90° 00'	-77° 00'	58° 28'	58° 21'
$\bar{8}805$	$\bar{1}23$	5° 05'	47° 46'	58° 19'	

Notes:

[1] These forms not observed.

[2] Corresponding to this the angle between the $[\bar{1}01]$ monoclinic axis, taken as c hexagonal and the [102] monoclinic axis, taken as $[21\bar{3}0]$ hexagonal is 90° 11 1/2'. The angle between c and a_2, hexagonal, is exactly 90° and corresponds to the angle between monoclinic b and c axes.

The angle between the monoclinic [010] and $[\bar{1}21]$ axes, corresponding to hexagonal a_2 and a_1, is 60° 4 1/2'.

The table is modified from the standard for monoclinic crystals in that the forms are listed in an order to emphasize the pseudorhombohedral character and by the substitution of angles other than those generally given for monoclinic crystals in the two columns at right.

The volume of the monoclinic cell is 1368.71 Å^3. The volume of the hexagonal cell for the pseudorhombohedral lattice, simulated by the association of monoclinic domains in three orientations turned at 120° to each other on the [102] axis, is just 12.0005 times greater. This close correspondence is to be expected, because small differences in spacing along the monoclinic [010] and $[\bar{1}21]$ axes, which correspond to a_2 and a_1 hexagonal, are effectively averaged in the rhombohedral interpretation. The calculated density with Z respectively 12 and 144 is 2.679 in either case. This may be compared with observed densities from Berman balance determinations:

kogarkoite (Lovozero massif)	2.66(6)[1] based on eight fragments with total weight 8.4 mg,
synthetic kogarkoite	2.67 (PS & S, Table 3), 2.666(6) six crystals grown from solution, 2.676(3) three fragments of crystals grown from melt.

[1] Here and in the rest of this article, the numbers in parentheses represent estimated standard deviations (e.s.d.) in terms of the least units cited for the value. Thus 2.676 (3) indicates an *e.s.d.* of 0.003 whereas 2.66 (6) indicates an *e.s.d.* of 0.06.

Morphology

Table 3 is a standard angle table for kogarkoite calculated from linear elements based on the monoclinic cell dimensions. Both monoclinic and hexagonal indices are listed. The indexing of de Marignac as given by Groth (1908, p. 376) and that of Foote and Schairer (1930, p. 4206) can be reconciled with the hexagonal indexing used here by interchanging designations of positive and negative rhombohedra and halving the $c:a$ ratio of the earlier authors, as previously explained by Pabst, Sawyer, and Switzer (1963, p. 496). The ρ angles only are given for the hexagonal description. In each case this angle lies within the range of the corresponding pair of monoclinic C angles. These relations are also shown in stereographic projection in Figure 3.

Since goniometric results were interpreted on the basis of a hexagonal reference system, only hexagonal indices will be used in the following discussion. All of the forms listed in Table 2 were reported by de Marignac. All of these forms have been repeatedly observed on synthetic crystals, both on crystals grown by Schairer and kindly supplied by him years ago and on crystals grown from solution in connection with the present study. The dominant forms are {0001}, $\{40\bar{4}1\}$ and $\{02\bar{2}1\}$, the faces of the latter two appearing on all crystals with about the same frequency. The frequency of $\{10\bar{1}1\}$ faces is less by a factor of about 2/7 and that of $\{80\bar{8}5\}$ faces by a factor of about 1/7.

There is a consistent difference in the habits of synthetic crystals and the natural crystals from Hortense Spring and Wright's well. The former are always tabular as shown by de Marignac (1859, Pl. IV, Fig. 9) and by Foshag (1931, Fig. 5). The natural crystals, however, lack the minor forms $\{10\bar{1}1\}$ and $\{80\bar{8}5\}$ and are of rhombohedral or bipyramidal habit, being rarely tabular. Figures 6A and 6B show four natural and four typical synthetic crystals. The synthetic crystals, being tabular, are all seen lying with *c* (hexagonal) normal to the plane of the picture. Two of the natural crystals are in this orientation but two have their *c* (hexagonal) axis parallel to the plane of the picture, showing the rhombohedral to bipyramidal habit. One of these shows a polar development which was seen on several crystals. Synthetic crystals were grown with dimensions up to 3.4 mm thick and 8.5 mm wide, but the mosaic structure of such large crystals is so pronounced that they are not suitable for measurement.

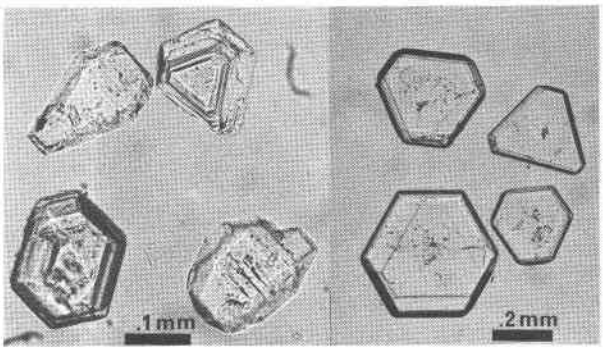

FIG. 6A and 6B. A (left) Four crystals of kogarkoite from Hortense Hot Springs, Colorado.
B (right) Four crystals of kogarkoite grown from solution.

Twinning

Possibly the almost omnipresent intergrowth previously discussed is to be considered a kind of twinning. de Marignac (1859) reported twinning on the base and Foote and Schairer (1930, p. 4206) reported that "twinning on the base is common." Such twinning is suggested by the appearance of faces of complementary rhombohedral forms simulating a nearly complete bipyramidal development. However, most of the measured synthetic crystals and a few of the natural crystals were found to have an ideal rhombohedral development with no suggestion of twinning. The twinning considered here corresponds to rotation of the rhombohedral lattice by 180° (or 60° or 300°) about the *c* axis (monoclinic [102]). It is easily recognized in *c* axis oscillation patterns, giving rise to an apparent symmetry plane normal to the oscillation axis, and in $(h0\bar{h}l)$ sections of the reciprocal lattice as well as in any higher layers normal to c^*. Patterns of some or all of these types were run on ten natural crystals and 10 synthetic crystals. All but one of the natural crystals show *X*-ray evidence of (0001) twinning. Contrary to the reports of previous observers, only one of the synthetic crystals was found to be a (0001) twin, this with the two parts of the twin of markedly unequal volume. Most of these crystals showed an ideal rhombohedral habit with no complementary forms.

Though (0001) twinning, which is widespread among truly rhombohedral crystals, was found to be infrequent in synthetic kogarkoite crystals grown from

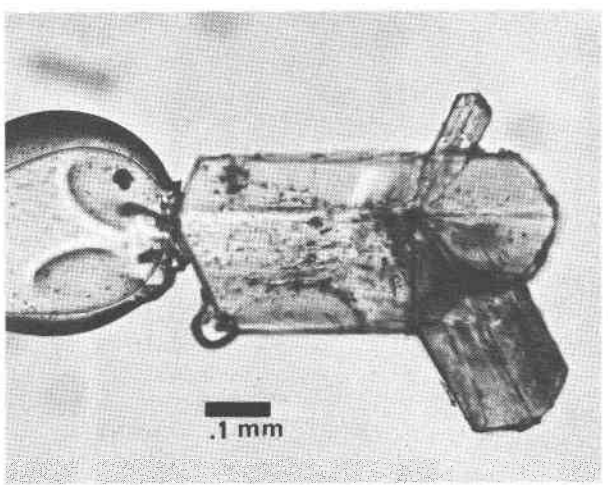

FIG. 7. Twin crystal of synthetic kogarkoite mounted for goniometry and X-ray diffraction. Photographed in immersion. Large horizontal face is (101) monoclinic, (0001) pseudohexagonal.

solution, it commonly occurred in pairs with an *a* (hexagonal) axis in common and the *c* axes inclined at about 58 1/2° to each other. About 25 such "twins" were found. Four were measured goniometrically and three of these, including one developed as a triplet and shown in Figure 7 as mounted for goniometry, were examined by $h0\bar{h}l$ precession photographs. In the best example, both parts of the twin are single crystals and the two are related by the approximate superposition of $(80\bar{8}5)$ on (0009). In another each of the diverging parts is in itself a (0001) twin. In the specimen shown in Figure 7, the main part is a (0001) twin and the satellites projecting on both sides are each turned on a common axis about 58 1/2° in opposite sense with respect to the main part.

Physical and Optical Properties

Hardness, determined on a large single crystal grown in suspension, can be given as 3 1/2+ but distinctly below 4, probably nearly the same as the hardness of schairerite, given as 3 1/2 by Foshag (1931, p. 135).

The melting point of Na_3SO_4F was given as 781°C by Wolters (1910, Table 3).

Foote and Schairer (1930, p. 4206) reported Na_3SO_4F to be "uniaxial, optically positive"; Wolters (1910, p. 67) reported it to be "nearly uniaxial, positive". Interference figures show broad isogyres due to the exceedingly low birefringence so that the very small optic angle cannot be measured. The crystals show no more spreading of the isogyres than do many crystals which must be considered truly uniaxial; however, they may show a bit of separation of the isogyres owing to strain or unknown causes. Even those few crystals that were found to be free or nearly free of the intergrowth which gives rise to the rhombohedral pseudosymmetry are essentially optically uniaxial so that the apparent uniaxial character cannot be ascribed to aggregate effects. Nevertheless, the optical properties as referred to the monoclinic axes should now be given as: $\alpha = \beta = 1.439(1)$, γ ($\perp\{101\}$) $= 1.442(1)$, $2V = 0°$ or very small. Birefringence, as determined by Berek compensator on two synthetic crystals, 0.36 and 0.33 mm thick, was found to be 0.0029(3). This is substantially higher than the birefringence, 0.0012(2), found for schairerite and for galeite (Pabst, Sawyer, and Switzer, 1963, Table 2). Direct comparison of kogarkoite from the Lovozero massif and from Colorado with synthetic kogarkoite showed that the refractive indices of all are identical.

Kogarkoite from the Lovozero massif was reported as 0.4 to 2 cm crystals that were "pale sky–blue in color" (Kogarko, 1961). No trace of color could be detected in the small crystals from Colorado, in any of the synthetic material, nor in small fragments of the Lovozero kogarkoite.

Phase Relations in the System Na_2SO_4–NaF–NaCl

Kogarkoite can be synthesized in several ways. de Marignac (1859) obtained it accidentally upon evaporating an HF solution of NaF, a bit of H_2SO_4 also being present. He found the double salt to be soluble in pure water from which it could be recrystallized by cooling. Wolters grew crystals from an aqueous solution at 35°C but found that at 20°C $Na_2SO_4 \cdot 10H_2O$ crystallizes first upon evaporation of an equimolal solution of Na_2SO_4 and NaF. Foote and Schairer (1930, Table 1) reported solubility isotherms in the system Na_2SO_4–NaF–H_2O at 10, 15, 25 and 35°C. They estimated that the lowest temperature at which Na_3SO_4F crystallizes in this system is 17.5°C. Their data for 25°C suggest that an aqueous solution containing 8.86 percent Na_2SO_4 and 2.37 percent NaF—this corresponds to a slight excess of Na_2SO_4 over the 1:1 proportion of Na_2SO_4:NaF—is in equilibrium with Na_3SO_4F and NaF; in other words, the saturation curve of NaF at 25°C in this system overlaps the point of equi-

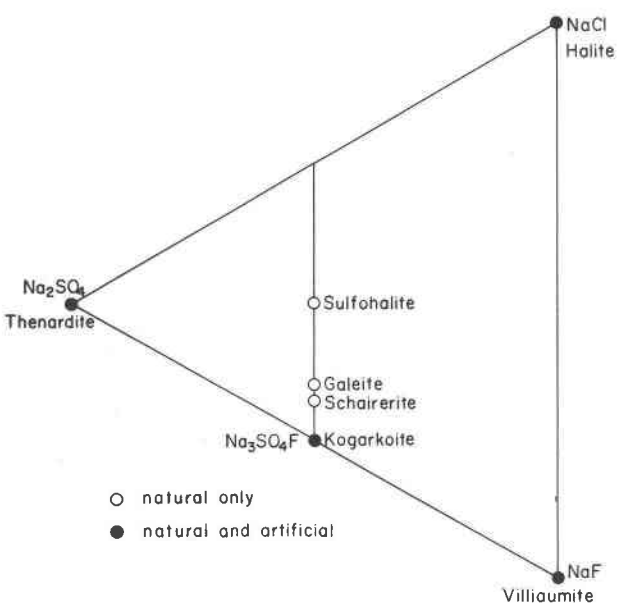

FIG. 8. Minerals in the system Na_2SO_4–NaF–NaCl. Compositions plotted in terms of mole proportions.

molal concentration of the two simple salts in solution. In the course of the present study, Na_3SO_4F was repeatedly crystallized from aqueous solution at 23°, at 38° and at 68°C without the appearance of NaF as a solid phase. The concentration of an aqueous solution saturated with Na_3SO_4F at 24°C was found to be 12.00(5) weight percent Na_3SO_4F, very close to the concentration under similar but not identical conditions reported by Foote and Schairer (1930, Table 1). The density of such a solution, as determined by a pycnometer of 10 cc capacity, is 1.11(1).

Besides being formed from a solution or from a melt (Wolters, 1910), kogarkoite can also be formed by sintering of NaF and Na_2SO_4 at 550°C or less. Further, it is formed topotactically with the separation of disoriented Na_2SO_4 and NaCl when schairerite, galeite, or sulfohalite are heated, the perfection of the alignment of the newly formed Na_3SO_4F varying inversely as the Cl content of the initial crystal (Pabst, Sawyer, and Switzer, 1963, pp. 508–509).

Wolters found no ternary salts in the system Na_2SO_4–NaF–NaCl and no one has reported synthesis of sulfohalite, $Na_6(SO_4)_2FCl$, nor of schairerite or galeite for which the formulas $Na_{21}(SO_4)_7F_6Cl$ $Na_{15}(SO_4)_5F_4Cl$ have recently been confirmed (Brown and Pabst, 1971).

Foote and Schairer (1930, p. 4215) stated that "in the quaternary system the double salt $Na_2SO_4 \cdot NaF$ has a limited part of its fluoride replaced by chloride" and that "The replacement of fluoride by chloride raises the indices of refraction of the double salt" but cited no measurements to support either statement. The diagram for the system Na_2SO_4–NaF–NaCl published with the description of galeite (Pabst, Sawyer, and Switzer, 1963, Fig. 6) included a solid line intended to indicate the range of composition of the solid solution reported by Foote and Schairer. This range overlapped the compositions of schairerite and galeite as plotted from the then available analyses, though even at that time Na_2SO_4F free of chlorine had been crystallized at room temperature from solutions containing NaF–NaCl in the ratio 4:1. Figure 8 is intended to replace the partly misleading figure of 1963. The line representing the supposed solid solution has been deleted and the points representing the compositions of schairerite and galeite have been replotted as required by reliable analyses and the newly confirmed formulas.

Structure

Evidence has been presented (Pabst, Sawyer, and Switzer, pp. 497–499) that the structures of galeite, schairerite, and kogarkoite are all related to that of sulfohalite (Watanabé, 1934; Pabst, 1934) which has recently been refined by Sakamoto (1968). This is indicated not only by the topotactic transformations and the dimensional relations among these phases but also by the close correspondence of X-ray diffraction intensity relations in the zone of the 3–fold or pseudo–3–fold axis (Pabst, Sawyer, and Switzer, 1963, Table 6). If referred to hexagonal axes, the structure of sulfohalite, as shown by Figure 8 in the same publication (except that a few Na atoms were inadvertently omitted from the drawing), suggests the hexagonal or rhombohedral structures of its close relatives.

Besides the rhombohedral pseudocell which arises in kogarkoite owing to the special dimensions of the monoclinic lattice, there is a smaller subcell within the monoclinic cell that is revealed by the intensity relations in the $\bar{h}2h\bar{h}l$ and $hk\bar{i}0$ sections of the hexagonal reciprocal lattice for the large rhombohedral pseudocell. Strong X-ray diffraction spots occur in photographs of the $\bar{h}2h\bar{h}l$ section only for $l = 9n$ and $h = 4n$ and in the $hki0$ section only for $h = 4n$. The strong spots correspond to a subcell for which c (hexagonal) is 8.155 Å and a (hexagonal) is 6.949, and indexed on this subcell they conform to rhombohedral centering of the hexagonal sublattice. The primitive rhombohedron has the dimensions a_r 4.846, α 91° 36′ and contains one formular unit of Na_3SO_4F. It corresponds closely to the one-eighth of the unit cube of face–centered sulfohalite which was pictured by Pabst (1934) and which may be considered a rhombohedron with a_r 5.034, and $\alpha = 90°\ 00'$, and cell content $Na_3SO_4F_{1/2}Cl_{1/2}$, there being F and Cl atoms at alternate corners of such a small cube (which is not a translation unit). A section through such a rhombohedron parallel to one of its symmetry planes is indicated by dotted lines at the right in Figure 9; this also shows the relation of this subcell to the monoclinic unit cell and to sulfohalite cells. In both parts of Figure 2 the dimensions of the hexagonal subcell are shown by dashed lines; those of the small rhombohedron within it, by dotted lines.

The rhombohedral subcell of kogarkoite has shrunken edges relative to the one-eighth unit cube of sulfohalite because of the smaller radius of F compared to Cl and is compressed along a body diagonal. A reasonable atomic arrangement can be

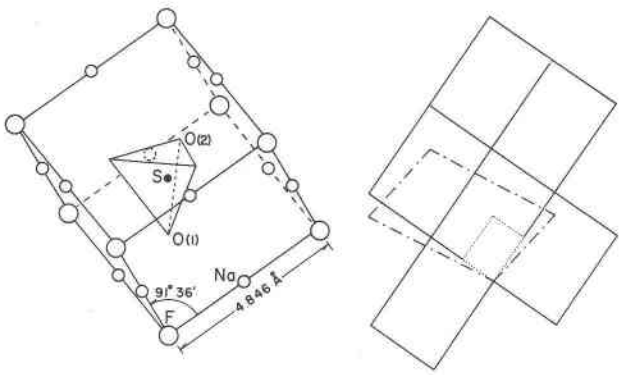

FIG. 9. (left) Atomic arrangement in pseudorhombohedral subcell in kogarkoite. Compare Omori (1970, Fig. 2) or Pabst (1934, Fig. 1). (right) Full lines, (110) sections of six unit cubes of sulfohalite; dot–dash lines, (010) section of monoclinic cell of kogarkoite; dotted lines, ($\bar{1}2.0$) section of pseudorhombohedral subcell of kogarkoite.

found within such a unit by analogy with the sulfohalite structure. F atoms are at the corners of the rhombohedron. Na atoms, which in sulfohalite are situated between F and Cl but displaced towards F, may be expected to be midway between two F atoms. Symmetry requires that S be at the center of the small cube in sulfohalite. If it were similarly placed in the deformed cube in Na_3SO_4F, distances between Na and the corners of the four nearest SO_4 groups would not be alike as they are in sulfohalite. However, it is easy to find a location and orientation of the SO_4 group such that these distances are equalized, dimensions for the SO_4 group being taken from Sakamoto's (1968) refinement of the sulfohalite structure. These considerations lead to a substructure shown at the left in Figure 9 and which may be described as shown in Table 4 where comparable data are also given for sulfohalite.

A table[1] records observed and calculated F's for 10 *hki*0 and 13 *hh*$\bar{2}\bar{h}l$ reflections for the subcell. For these *R* is just under 24 percent. This may be taken to confirm the expectation that near-neighbor relations in kogarkoite are similar to those in sulfohalite. However, the subcell structure is based on relations in two projections only. Many of the strong spots seen in the two patterns shown on Figure 4 cannot be accounted for in terms of this subcell. So the subcell cannot be considered an approximation to a translation unit. If the true space group is indeed $P2_1$ or $P2_1/m$, as systematic absences suggest, SO_4 groups must be present in at least two orientations as they are in sulfohalite.

TABLE 4. DATA FOR STRUCTURE OF THE RHOMBOHEDRAL SUBCELL OF KOGARKOITE AND THE CORRESPONDING ONE EIGHTH UNIT CUBE OF SULFOHALITE

	kogarkoite			sulfohalite		
a_r	4.846 Å			5.034		
α	91° 48'			90° 00'		
Z	Na_3SO_4F			$Na_3SO_4\frac{FCl}{2\,2}$		
R3m		x	z		x	z
F in 1 a	x,x,x	0		F,Cl	0	
S in 1 a		0.496			0.500	
O_1 in 1 a		0.315			0.331	
3 O_2 in 3 b	x,x,z	0.671	0.325		0.662	0.331
3 Na in 3 b		0.500	0.000		0.446	0.000
S - O		1.474			1.474	
Na - O		2.343			2.430	
Na - F		2.423			2.247	(Na - Cl 2.787)
O_1 - F		2.604		O - F	2.886	
O_2 - F		2.773		O - Cl	4.110	

Data for sulfohalite derived from Sakamoto (1968, table 3)

The subcell structure suggests that sheets of F atoms parallel to (0001)—(101) monoclinic—occur at intervals of 8.155/3 = 2.718 Å. The slightly larger value, 2.722, used by Brown and Pabst (1971, p. 177) in predicting cell dimensions for galeite and schairerite was based on the *c* dimension previously reported for this phase. Substitution of the improved value for the distances between the fluorine sheets would reduce the "c_h predicted" by 0.012 and 0.020 respectively, slightly improving the agreement between observed and predicted cell dimensions of galeite and schairerite.

Acknowledgments

We are indebted to Drs. E. Roedder and M. Fleischer for their aid in securing a bit of kogarkoite from the Lovozero massif. Most of the photographic work for this report was done by Mr. J. Hampel. Parts of this study have been supported by research funds of the Department of Geology and Geophysics, University of California, Berkeley.

[1] A table listing observed and calculated structure factors for the subcell structure of kogarkoite shown in Figure 9, for *hki*0 and *hhil* only, may be obtained by writing A. Pabst.

References

BROWN, F. H., AND A. PABST (1971) New data on galeite and schairerite. *Amer. Mineral.* **56,** 174–178.

FOOTE, H. W., AND J. F. SCHAIRER (1930) The system Na_2SO_4–NaF–NaCl–H_2O. *J. Amer. Chem. Soc.* **52,** 4202–4217.

FOSHAG, WILLIAM F. (1931) Schairerite, a new mineral from Searles Lake, California. *Amer. Mineral.* **16,** 133–139.

GROTH, P. (1908) *Chemische Krystallographie, Vol. 2.* Engelmann, Leipzig.

KOGARKO, L. N. (1961) Chlorine-free schairerite from the nepheline syenites of the Lovozero massif (Kola Peninsula). *Dokl. Akad. Nauk. SSSR,* **139,** 435–437 (in Russian). [trans. *Dokl., Earth Sci. Sec.* **139,** 839–841 (January, 1963)].

DE MARIGNAC, CH. (1859) Recherches sur les formes cristallines et la composition chimique de divers sels. *Ann. des Mines,* **15,** 221–290.

OMORI, KEIICHI (1970) Infrared study of sulfohalite. *Amer. Mineral.* **55,** 1897–1910.

PABST, ADOLF (1934) The crystal structure of sulphohalite. *Z. Kristallogr.* **89,** 514–517.

PABST, ADOLF, D. L. SAWYER, AND GEORGE SWITZER (1963) Galeite and related phases in the system Na_2SO_4–NaF–NaCl. *Amer. Mineral.* **48,** 485–510.

SAKAMOTO, YOSIO (1968) The size, atomic charges, and motion of the sulfate radical of symmetry $\bar{4}3m$ in the crystal of sulfohalite, $Na_6ClF(SO_4)_2$. *J. Sci. Hiroshima Univ., Ser. A–II,* **32,** 101–108.

SHARP, WILLIAM N. (1970) Extensive zeolitization associated with hot springs in central Colorado. *U.S. Geol. Surv. Prof. Pap.* **700–B,** B14–B20.

WATANABÉ, TOKONOSUKÉ (1934) The crystal structure of sulphohalite. *Proc. Imperial Acad. (Japan),* **X,** 575–577.

WOLTERS, ADOLF (1910) Das ternäre System Na_2SO_4 + NaFl + NaCl. *Neues Jahrb. Mineral. Beil.–Bd.* **30,** 55–96.

Manuscript received, July 19, 1972; accepted for publication, September 15, 1972.